High-Resolution Specification of the Land and Ocean Surface for Improving Regional Mesoscale Model Predictions

Jonathan L. Case[1], Steven M. Lazarus[2], Michael E. Splitt[2], William L. Crosson[3],
William M. Lapenta[4], Gary J. Jedlovec[4], and Christa D. Peters-Lidard[5]

[1]ENSCO Inc./Short-term Prediction Research and Transition (SPoRT) Center
320 Sparkman Dr., Huntsville, AL 35805
Voice: 256.961.7504
Fax: 256.961.7788

[2]Florida Institute of Technology, Melbourne, FL
[3]Universities Space Research Association, Huntsville, AL
[4]NASA Marshall Space Flight Center/SPoRT Center, Huntsville, AL
[5]NASAGoddard Space Flight Center, Greenbelt, MD

The exchange of energy and moisture between the Earth's surface and the atmospheric boundary layer plays a critical role in many meteorological processes. High-resolution, accurate representations of surface properties such as sea-surface temperature (SST), soil temperature and moisture content, ground fluxes, and vegetation are necessary to better understand the Earth-atmosphere interactions and improve numerical predictions of sensible weather. The NASA Short-term Prediction Research and Transition (SPoRT) Center has been conducting separate studies to examine the impacts of high-resolution land-surface initialization data from the Goddard Space Flight Center Land Information System (LIS) on subsequent WRF forecasts, as well as the influence of initializing WRF with SST composites derived from the MODIS instrument. This current project addresses the combined impacts of using high-resolution lower boundary data over both land (LIS data) and water (MODIS SSTs) on the subsequent daily WRF forecasts over Florida during May 2004.

For this experiment, the WRF model is configured to run on a nested domain with 9-km and 3-km grid spacing, centered on the Florida peninsula and adjacent coastal waters of the Gulf of Mexico and Atlantic Ocean. A control configuration of WRF is established to take all initial condition data from the NCEP Eta model. Meanwhile, two WRF experimental runs are configured to use high-resolution initialization data from (1) LIS land-surface data only, and (2) a combination of LIS data and high-resolution MODIS SST composites. The experiment involves running 24-hour simulations of the control WRF configuration, the LIS-initialized WRF, and the LIS+MODIS-initialized WRF daily for the entire month of May 2004. All atmospheric data for initial and boundary conditions for the Control, LIS, and LIS+MODIS runs come from the NCEP Eta model on a 40-km grid. Verification statistics are generated at land surface observation sites and buoys, and the impacts of the high-resolution lower boundary data on the development and evolution of mesoscale circulations such as sea and land breezes are examined. This paper will present the results of these WRF modeling experiments using LIS and MODIS lower boundary datasets over the Florida peninsula during May 2004.

13.5   HIGH-RESOLUTION SPECIFICATION OF THE LAND AND OCEAN SURFACE FOR
IMPROVING REGIONAL MESOSCALE MODEL PREDICTIONS

Jonathan L. Case*[1], Geoffrey T. Stano[1], Michael E. Splitt[2], Steven M. Lazarus[2],
William L. Crosson[3], William M. Lapenta[4], Gary J. Jedlovec[4], and Christa D. Peters-Lidard[5]

[1]ENSCO Inc./Short-term Prediction Research and Transition (SPoRT) Center, Huntsville, AL
[2]Florida Institute of Technology, Melbourne, FL
[3]Universities Space Research Association, Huntsville, AL
[4]NASA Marshall Space Flight Center/SPoRT Center, Huntsville, AL
[5]NASA Goddard Space Flight Center, Greenbelt, MD

1. INTRODUCTION

The exchange of energy and moisture between the Earth's surface and the atmospheric boundary layer plays a critical role in many meteorological processes. High-resolution, accurate representations of surface properties such as sea-surface temperature (SST), soil temperature and moisture content, ground fluxes, and vegetation are necessary to better understand the Earth-atmosphere interactions and improve numerical weather prediction (NWP) of sensible weather. In coastal zones that are influenced by both land-atmosphere and sea-atmosphere interactions, it is important to accurately specify the land and ocean surface in order to simulate realistic atmospheric phenomena in NWP models.

The NASA Short-term Prediction Research and Transition (SPoRT) Center has been conducting separate studies to examine the impacts of high-resolution land-surface initialization data from the Goddard Space Flight Center Land Information System (LIS, Kumar et al. 2006, 2007a) on subsequent NWP forecasts (Case et al 2007a), as well as the influence of initializing an NWP model with SST composites derived from the Earth Observing System (EOS) Moderate Resolution Imaging Spectroradiometer (MODIS) instruments aboard the Aqua and Terra satellites (Haines et al. 2007; LaCasse et al. 2007). Here, the authors examine the combined impacts of using high-resolution lower boundary data over both land and water on daily NWP forecasts over Florida during May 2004. Using the Weather Research and Forecasting (WRF) model in conjunction with the LIS land surface and MODIS SST initialization data, the objective of this project is to evaluate the impacts of these high-resolution lower boundary data on regional short-term NWP (0–24 hours). The ultimate goal of this and other SPoRT projects is to accelerate the infusion of NASA Earth Science observations, data assimilation and modeling research into National Weather Service forecast operations and decision-making at the regional and local level.

This paper provides a description of the experiment design and presents preliminary results from WRF runs using the both LIS and MODIS data in the initial conditions. The remainder of the paper is organized as follows. Sections 2 and 4 provide background information on the LIS software and the MODIS SST composite product. The experiment design is presented in Section 3 with preliminary results given in Section 6. Sections 7–9 consist of the summary, acknowledgements, and references, respectively.

2. LAND INFORMATION SYSTEM (LIS)

LIS is a software framework that integrates satellite-derived datasets, ground-based observations and model reanalyses to force a variety of land surface models (LSMs). By using scalable, high-performance computing and data management technologies, LIS can run LSMs offline globally with a grid spacing as fine as 1 km to characterize land surface states and fluxes. The software infrastructure enables LIS to ingest high-resolution datasets such as leaf area index and vegetation fraction derived from the MODIS instruments on the Terra and Aqua satellites. LIS has been used to demonstrate land surface modeling capability at 1-km grid spacing over urban areas (Peters-Lidard et al. 2004), and also has the ability to assimilate land surface observations using techniques such as Ensemble Kalman Filtering (Kumar et al. 2007b).

To predict water and energy processes, LSMs require (1) initial conditions, (2) boundary conditions from the atmosphere (i.e. forcings such as temperature, precipitation, radiation, wind, etc.) and lower soil states, and (3) parameters describing the soil, vegetation, topography, and other surface properties. Using these inputs, LSMs solve the governing equations of the soil-vegetation-snowpack medium, and predict surface fluxes and soil states in order to provide a realistic representation of the transfer of mass, energy, and momentum between the land surface and the atmosphere (Kumar et al. 2006).

By itself, LIS runs in an uncoupled, offline mode using a variety of atmospheric forcings such as the Global Data Assimilation System (GDAS, Derber et al. 1991), the North American Land Data Assimilation System (NLDAS, Mitchell et al. 2004), and supplemental precipitation data. These forcings are used to drive one of several community LSMs available in LIS: the Noah LSM, the CLM, the Variable Infiltration Capacity model (VIC, Liang et al. 1994, 1996), the Mosaic model (Koster and Suarez 1996), and the SiB model with Hydrology (Sellers et al. 1986; Sud and Mocko 1999).

*Corresponding author address: Jonathan Case, ENSCO, Inc., 320 Sparkman Dr., Room 3062, Huntsville, AL, 35805. Email: Jonathan.Case-1@nasa.gov

In addition to running offline, LIS can also be run in a coupled mode with WRF to integrate surface and soil quantities using the LSMs available in LIS. The LIS has been coupled to the Advanced Research WRF (ARW, Skamarock et al. 2005), giving users the ability to run an ensemble system of LSMs within the ARW dynamical core (Kumar et al. 2007a). WRF atmospheric forcing is imported to a coupled version of the LIS which then runs a user-selected LSM. The LSM output is then exported back to the WRF code in the form of soil temperature, moisture, surface fluxes, etc. Diagnostic variables (such as 2-m temperature and dewpoint) are calculated within the WRF code following the call to LIS. This setup allows users to run the same LSM configuration in the WRF simulation as was designed in the offline LIS run.

The benefits of running LIS with WRF for regional modeling are numerous. First, LIS provides the capability to conduct long-term offline integrations or "spinups" to allow the surface and soil profiles to reach thermodynamic equilibrium, using bias-adjusted meteorological inputs or "forcings". Producing high-resolution spinups is not currently possible using the standard WRF version, and therefore most users initialize surface and soil fields by interpolating from a coarser-resolution analysis/forecast system such as GDAS or the North American Mesoscale model. However, recent work by Chen et al. (2007) and Rodell et al. (2005) have shown that changing soil types from a coarse-resolution analysis system to a fine-scale regional forecast grid may require spinup times in excess of two years, particularly for high latitude or high elevation areas. Second, offline LIS output is generated at the same resolution as the local/regional grids (i.e. for each nest), and is then used directly as input to the WRF simulation, eliminating the need for horizontal spatial interpolation of land-surface variables from a larger-scale NWP model. Third, users can run WRF with the LSMs available in LIS, whereas only the Noah, Rapid Update Cycle's LSM, or thermal diffusion scheme can be run within the standard ARW. Finally, the LIS provides a plug-in framework through which users can introduce new high-resolution land datasets, LSMs, or land surface observations into WRF.

3. ETA MODEL SST PRODUCT

The NCEP Eta model began using a daily SST two-dimensional variational analysis (2D-VAR), provided by the NCEP Ocean Modeling Branch (OMB), in January 2001 to set the initial SSTs. This dataset is designed specifically to better resolve

- SST gradients around warm and cold ocean currents,
- Great Lakes surface temperatures and ice cover,
- Monthly climatology for the Great Salt Lake from the Saltair Boat Harbor (Steenburgh et al. 2000); the Salton Sea, CA; and the Fort Peck Reservoir, MT, and
- Cold continental shelf waters found adjacent to continents in winter.

The NCEP Eta model has been demonstrated to have high sensitivity to how the initial SSTs are

prescribed for coastal cyclogenesis location and timing and the associated precipitation patterns, and precipitation generated by the model over the Great Lakes. The initial SSTs are kept constant as the Eta forecast evolves (which will not be true in strong cold outbreak events). The analysis is available at 0000 UTC at 0.5° x 0.5° resolution and is interpolated to the NCEP Eta grid. More detailed information on the OMB 2-D VAR SSTs and current water surface temperature conditions is available through the NCEP's Ocean Modeling Branch Web page at http://polar.ncep.noaa.gov/Welcome.html.

4. MODIS SST COMPOSITE PRODUCT

A 1-km MODIS SST composite, produced at the NASA Short-term Prediction Research and Transition (SPoRT) Center, was created by combining multiple passes of the EOS MODIS SST data (Haines et al. 2007). The compositing assumes that the day-to-day variation of SST is relatively small — the degree to which this assumption is valid will likely vary spatially and seasonally. Data from both the Terra and Aqua platforms were combined to create separate day/night composites. The composites were created using the five most recent clear-sky SST values for each pixel. Daytime (nighttime) passes through the composite region occur at approximately 1600 and 1900 UTC. (0400 and 0700 UTC), respectively. The compositing method used the warmest three of the five pixels in order to mitigate the impact of cloud contamination.

Prior to being interpolated to the WRF grid, the 1-km MODIS SST composite was sub-sampled to a coarser grid with the same resolution as the finest WRF domain (i.e. 3-km grid spacing; the WRF domain configuration is discussed further in Section 5.2). Also, only the Aqua composites at 1900 and 0700 UTC were used in this study to initialize twice daily WRF simulations at 0000 and 1200 UTC, respectively. This configuration was designed to emulate a possible operational mode.

5. EXPERIMENT DESIGN

The experiment design consists of evaluating a set of Control WRF simulations using land surface and SST data initialized from the NCEP Eta model versus the following configurations of WRF:

- Simulations initialized with land surface data provided by the LIS software and Eta model SSTs (hereafter 'LISWRF'),
- Simulations initialized with MODIS SSTs in addition to the LIS land surface data (hereafter 'LISMOD').

Details of the period of record, WRF model configuration, and offline LIS run are provided in the sub-sections that follow.

5.1 May 2004 Weather Conditions over Florida

Experiments were conducted during May 2004 because the majority of this month experienced relatively quiescent large-scale weather conditions over the region of interest, which enabled us to focus on the local and mesoscale impacts of the high-resolution land

surface and SST initial conditions on predictions of 2-m air temperatures and dewpoint temperatures, 10-m winds, surface energy fluxes, and sea-breeze development. The minimal precipitation during this month allowed for an extended dry-down of the soil, which is critical to capture the soil moisture dynamics and hence the impacts of soil initialization.

A surface frontal passage associated with pre-frontal precipitation occurred from 1–4 May followed by clear, dry and relatively light synoptic winds from 5–8 May. A prolonged period of relatively strong easterly flow occurred from 9–19 May accompanied by periodic clouds and showers. The synoptic flow became more light and variable from 20–23 May, and then more westerly from the 25th through the rest of the month. Pre-frontal convection occurred over north Florida and south Georgia on the afternoon of the 31st.

5.2 WRF Configuration

The simulation domain (depicted in Figure 1) consists of two grids with 9-km and 3-km horizontal grid spacing. Both grids contains 43 sigma-pressure vertical levels from near the surface to a domain top at 75 mb, with a minimum vertical spacing of approximately 65 m near the surface.

For all three sets of simulations (Control, LISWRF, and LISMOD), the ARW dynamical core was used along with physics options consisting of the rapid radiative transfer model (Mlawer et al. 1997) and the Dudhia scheme (Dudhia 1989) for longwave and shortwave radiation, respectively. The WRF Single Moment 6-class microphysics scheme (WSM6, Hong et al. 2004; Skamarock et al. 2005) is used in conjunction with the modified Kain-Fritsch convective parameterization scheme (Kain 2004) on the 9-km grid, and without any convective parameterization on the 3-km inner nested grid. The planetary boundary layer and turbulence processes are parameterized by the Mellor-Yamada-Janjić scheme (Janjić 1990, 1996, 2002). Surface-layer calculations of friction velocities and exchange coefficients needed for the determination of sensible and latent fluxes in the LSM are provided by the NCEP Eta similarity theory scheme (Janjić 1996, 2002). Horizontal diffusion is handled by the two-dimensional Smagorinsky first-order closure scheme (Smagorinsky et al. 1965). All WRF runs used the Noah LSM as configured in version 2.1.2 of the ARW.

5.3 Offline LIS Spin-up Simulation

For the offline simulation, the Noah LSM was used in LIS version 4.3 with atmospheric forcings provided by NLDAS analyses (and GDAS analyses outside of the NLDAS coverage region). The NLDAS consists of hourly atmospheric analysis data over North America at 0.125° (~14 km) horizontal resolution. The GDAS has global coverage, but with six-hourly analyses at a coarser horizontal resolution of 0.469° (~52 km).

The offline LIS was run for 2 years and 1 month from 1 May 2002 to 1 June 2004, using a timestep of 30 minutes for integrating the Noah LSM. The process of determining an appropriate offline simulation length for achieving soil-state equilibrium for this experiment is described in Case et al. (2007b). In this study, the

authors found that a 9-month integration length was adequate for bringing the LSM into equilibrium for most of the Florida peninsula. This integration time is relatively short compared to that required for other domains because the porous nature of the predominantly sandy soil over Florida, combined with its subtropical climate and frequent precipitation, allows the soil moisture to adjust more rapidly to atmospheric forcing. This relatively short required spinup time is consistent with the results of Chen et al. (2007).

However, due to the extent of the nested grid configuration and for the purposes of optimizing initial land surface conditions in the LISWRF and LISMOD experiments, we increased the offline integration of the Noah LSM in LIS to 2 years prior to initializing the land surface variables. The additional run time ensures convergence to a soil-state equilibrium, particularly on the outer 9-km grid. The outer grid contains many different soil types in addition to sandy soils, thereby requiring a longer integration time frame to reach an equilibrium soil state compared to that found in Case et al. (2007b) for the Florida sub-domain.

The outer 9-km grid utilized the Zobler 9-class global soil scheme (Zobler 1986), which employs the global soil database from the United Nation's Food and Agriculture Organization within version 2.6 of the Noah LSM. Meanwhile, the inner 3-km nested grid used the State Soil Geographic (STATSGO, Miller and White 1998) database, valid only over the Continental U.S. The STATSGO soil texture database contains 19 classes of soil characteristics and is nearly the same as the database used in the ARW version 2.1.2. For the land-water mask and land cover, the U.S. Geological Survey (USGS) 1-km global database derived from the Advanced Very High Resolution Radiometer (AVHRR) satellite data from 1992–1993 was interpolated to the 9-km and 3-km grids. This land cover dataset is the same as that used in the ARW.

Additional required parameters that were used in the offline LIS runs include quarterly climatologies of albedo (Briegleb et al. 1986), maximum snow-free albedo (Robinson and Kukla 1985), and monthly climatologies of greenness fraction data derived from the AVHRR satellite (Gutman and Ignatov 1998). A deep soil temperature climatology provided a lower boundary condition for the soil layers at 3 meters below ground, and was derived from 6 years of GDAS 3-hourly averaged 2-m air temperatures using the method described in Chen and Dudhia (2001).

5.4 Control, LISWRF, and LISMOD experiments

Twenty-four hour simulations of the Control, LISWRF, and LISMOD configurations were run daily for the entire month of May 2004, except for the 24th and 28th when archived atmospheric boundary condition data were missing. Soil initial conditions in the Control runs were obtained through a spatial interpolation of the soil temperature and moisture values from the NCEP Eta model data (projected onto a 40-km grid) to the 9-km and 3-km grids, using the WRF Standard Initialization (WRFSI) utilities. The SSTs from the NCEP Eta data were interpolated to the WRF grids for the Control and LISWRF simulations, also using the WRFSI utilities.

All atmospheric data for initial and boundary conditions for each experiment came from 0–24 h forecasts from the 0000 UTC and 1200 UTC forecast cycles of the 40-km NCEP Eta model data, respectively. The Eta model provided boundary conditions to the 9-km grid every 3 hours, while the 9-km simulation grid provided boundary conditions every model timestep to the 3-km grid in a one-way nest.

Output from the offline LIS run was used to initialize the land surface fields in the LISWRF and LISMOD runs at both 0000 UTC and 1200 UTC every day during May 2004. The LIS software was called in the first model timestep to initialize the land surface variables with the LIS output. For the remainder of the integration, the Noah LSM within the standard ARW configuration was called. Therefore, the only differences between the Control and LISWRF simulations are those that resulted from differences in the land/soil conditions in the first model timestep. Land surface data interpolated from the 40-km Eta grids were used to initialize the Control runs while the spun-up LIS data on the simulation grids were used to initialize the LISWRF runs.

In the LISMOD runs, the MODIS SST composites sub-sampled to a 3-km resolution grid were interpolated to the WRF grids using the WRFSI utilities. Since the SSTs remained static throughout the model integration, the only differences between the LISWRF and LISMOD runs are those that resulted from differences in the SST state (NCEP Eta vs. MODIS). All evaluations, comparisons, and verification were done on the inner 3-km grid.

6. PRELIMINARY RESULTS

6.1 Impact of Land Surface Initialization: 6 May Sea Breeze Case

The sensitivity simulation from 1200 UTC 6 May 2004 is a good example of how the land surface initialization can impact the atmospheric sensible weather on a clear day. The initial 0–10 cm volumetric soil moisture difference field between the LISWRF and Control at 1200 UTC 6 May (Figure 2) indicates that LIS is drier than the Control (i.e. Eta model values) by more than 10% over parts of north Florida, southwestern Georgia, and the Bahamas, with a smaller magnitude of drying over a large portion of the Florida peninsula. LIS is more moist by 2–8% over southeastern Georgia and extreme south Florida near the Everglades. These soil moisture differences closely follow the pattern of soil texture across the domain (not shown), as the drying of the soils is largely controlled by soil type and corresponding hydraulic properties (Chen et al. 2007).

The drier initial LIS soil fields over north Florida impacted the evolution of the simulated sea-breeze fronts on 6 May. Figure 3a shows a noticeable separation between the LISWRF and Control sea-breeze fronts at the 11-hour forecast near Perry, FL (40J, highlighted in Figure 3a), with the LISWRF sea-breeze front (colored) having advanced further inland relative to the Control sea-breeze front (gray shaded). This inland penetration difference is consistent with the increased land-sea temperature contrast that can be inferred from the LISWRF run, based on the 1–3°C

positive differences in predicted 2-m temperatures over a large portion of north Florida (LIWRF – Control, Figure 3b). The narrow band of negative differences in predicted 2-m temperatures close to the coast indicates the greater penetration of post-sea-breeze marine air in the LISWRF run relative to the Control simulation.

At 40J, the LISWRF daytime forecast 2-m temperatures began about the same as in the Control run, but warmed much more quickly than the Control and stayed at least a few degrees warmer through 2200 UTC (Figure 4, top panel). In addition, the LISWRF 2-m dewpoints were several degrees lower than the Control 2-m dewpoints between 1300 UTC and 2100 UTC, almost exactly the same as the observed 2-m dewpoints during those hours (second panel in Figure 4). Based on these results, it can be inferred that the lower LISWRF soil moisture near 40J is more representative due to the improved 2-m temperature and dewpoint forecasts during much of the daylight hours.

A noteworthy feature at 40J is the improved timing of the sea-breeze passage in LISWRF compared to the Control. The sea-breeze passage is accompanied by an increase in 2-m dewpoints and 10-m wind speed, and a shift to a southwesterly wind direction. According to the observed traces (dashed lines), the observed sea-breeze passage occurred at about 2100 UTC (Figure 4). Meanwhile both the Control and LISWRF simulated the sea-breeze frontal passage too late at 40J. However the sea-breeze onset occurred one hour earlier in the LISWRF (2200 UTC) relative to the Control (2300 UTC), closer to the observed timing at 2100 UTC.

The 6 May case helps to illustrate the impact of the drier initial soil moisture over north Florida and south Georgia in the LISWRF simulation. The pattern of warmer LISWRF 2-m temperatures in Figure 3b correlates closely with the pattern of drier 0–10 cm soil moisture in Figure 2. Consequently, a larger land-sea temperature contrast exists across the portion of north Florida where the LISWRF sea breeze is seen to penetrate inland more rapidly than in the Control simulation.

This example of improved sea-breeze timing indicates that the higher-resolution land surface initial conditions of LISWRF can have a favorable impact on sensible weather features in a coastal region experiencing a quiescent environment. The authors are in the process of examining the sea-breeze timing at additional stations and days during May 2004 to quantify the net improvement of the high-resolution LIS/Noah land-surface initialization on the sea-breeze forecast accuracy in WRF. Improved sea-breeze prediction in coastal zones has implications on potential improvements to predictions of summertime convective initiation over such regions, which could be a follow-on phase of this current study.

6.2 SST Initialization Impacts

A sample difference fields comparing the Eta model SSTs to the MODIS SSTs for the 1200 UTC 6 May model initialization is given in Figure 5. The SSTs interpolated from the 40-km Eta model data (Figure 5a) has much smoother transitions than the more detailed

MODIS SST composite interpolated to the WRF grid (Figure 5b). An examination of the difference field shows that the MODIS SSTs are cooler by up to 3°C over the shallow shelf waters near the Florida east coast, while a narrow ribbon of slightly warmer SSTs are found within the Florida Current (i.e. Gulf Stream) to the east of the peninsula (Figure 5c). Other less systematic variations occur throughout the rest of the domain. In general, a greater coverage of cooler SSTs are found in the MODIS fields compared to the Eta SSTs at this particular time.

Little change occurred to the predicted sea breezes from the 6 May case when including the high-resolution MODIS SSTs (not shown). In fact, the overall impact of the MODIS SSTs on sea breezes during May 2004 was quite minimal. The heating over land is the primary driver of sea breeze development and evolution, which is not significantly impacted by changes in SSTs offshore.

LaCasse *et al.* (2007) provide a thorough analysis of the impacts of the high-resolution MODIS SST composite on the WRF predictions during May 2004. Their general conclusions are that model predictions using the MODIS SST data resulted in enhanced convergence zones, stronger horizontal convective rolls, an increase and displacement of precipitation systems, and slight improvements in wind speed over the ocean. The next section provides some composite verification statistics over both land and water stations quantifying the changes in verification statistics when using the LIS initial land surface data with and without the MODIS SSTs.

6.3 Surface Verification

Surface verification statistics were computed *separately over land sites (METAR and FAWN) and* marine sites (buoy and C-MAN) as depicted in Figure 6. The composite statistics for land and marine sites are presented for the 0000 UTC forecast cycle in Figure 7 and Figure 8, respectively.

In general, the most significant improvements in surface errors were with the land sites associated with the addition of LIS land surface initialization data in the LISWRF experiment. Based on the hourly 2-m temperature errors at land stations (Figure 7a), the LISWRF clearly improves upon the Control predictions. The LISWRF RMSE is a few tenths of a degree Celsius smaller than the Control at nearly all forecast hours, primarily due to a reduction of the nocturnal warm bias from hours 0–11 and a reduction in the daytime cool bias from hours 16–23. This improved diurnal range in predicted 2-m temperatures can be attributed to the lower soil moisture initial conditions in the LISWRF compared to the Control, resulting in a greater partitioning of sensible heat flux in the overall energy budget. The additional of the high-resolution MODIS SSTs (LISMOD plot) produced very little change in the 2-m temperature errors over land.

Despite the improvements seen in the simulated 2-m temperatures, very little overall improvement occurs in the 2-m dewpoint errors (Figure 7b). Between hours 0–15, the RMSE and biases are quite similar. Thereafter, the biases drift apart with the Control

becoming slightly too moist by hour 20, while the LISWRF retains a small dry bias (-0.2 to -0.5°C) from hours 15–20, and then realizes a nearly unbiased 2-m dewpoint from hours 21–24 (Figure 7b). Once again, the LISMOD errors are nearly the same as the LISWRF errors.

The wind speed errors indicate that LISWRF improved slightly over the Control during the nighttime hours (Figure 7c). Between forecast hours 0 and 12, the RMSE is lower by a few tenths of a meter per second during most hours. Once again, the total error reduction can be attributed to a reduction in the bias. Both the Control and LISWRF experience a positive bias in the wind speed during all forecast hours; however, during the nocturnal hours, the LISWRF improves upon the Control bias until forecast hour 11. Between hours 21–24, the LISWRF has a slightly higher positive wind speed bias, possibly due to stronger post-sea-breeze *winds at numerous coastal locations, given the larger* land-sea temperature contrast of LISWRF. Only very small variations are found between the LISWRF and LISMOD errors over land stations.

The 10-cm soil temperature forecasts tend to be too cold relative to the FAWN sites during most forecast hours in both the Control and LISWRF (Figure 7d). The LISWRF is even colder on average than the Control by as much as 1.5°C during the nighttime hours, as noted by the differences in biases from 0–11 hours. This result is most likely due to the handling of downward shortwave radiation forcing in the NLDAS analyses. As described in Mitchell *et al.* (2004), the NLDAS obtained all its forcing from the Eta Data Assimilation System (EDAS), except for the downward shortwave radiation. Due to ~10–20% high biases in shortwave radiation in the EDAS/Eta model (Betts *et al.* 1997), the NLDAS instead utilizes GOES-based solar insolation as the primary downward shortwave radiation forcing. The lower values of NLDAS downward shortwave radiation help explain why the LISWRF soil temperatures are colder than the Control (Eta) values at the 0000 UTC initialization. During the daytime hours (12–24 hours), the Control and LISWRF biases converge to -2°C by 24 hours. As a result of the increase in the negative bias, the magnitude of the LISWRF RMSE exceeds the Control during all forecast hours. As expected, virtually no difference occurs between the LISWRF and LISMOD forecast 10-cm soil temperatures.

The 0000 UTC surface verification statistics computed at the marine sites of Figure 6 indicate generally nominal changes in errors when including the MODIS SSTs. In general, only small variations in errors occurred in the 2-m temperature, dewpoint, and 10-m wind speed (Figure 8a-c). The most substantial *differences between the Control, LISWRF, and LISMOD* are found in the SST errors (Figure 8d), where the LISMOD bias show systematically cooler SSTs by a few tenths of a degree Celsius compared to the LISWRF and Control (i.e. Eta model SSTs). The RMSE is nearly the same for the Eta and MODIS. Note that the SSTs are verified at only a few point locations and therefore may not be representative of the overall differences between the Eta and MODIS SSTs. Similar results were seen in the *1200 UTC errors (not shown).*

It is interesting to note the diurnal trend in the SST bias during the 24 forecast hours, prevalent in both the Control/LISWRF and LISMOD runs. Since the SSTs are fixed in each WRF simulation, this result depicts the monthly-averaged diurnal component to the observed SSTs at these select locations during May 2004. The SST biases begin slightly below 0, reach a maximum by 1200 UTC (corresponding to a minimum in observed SST), and then decrease to a minimum at ~2100 UTC (corresponding to the maximum observed SST), with an amplitude between 0.5°–1.0°C. This result suggests that it may be important to capture SST variations in local modeling applications, even on diurnal temporal scales. Since the MODIS SST composites are available up to 4 times per day at a given location, this NASA resource could be used in local and regional modeling applications to capture some of the diurnal variability in the SST not currently available in other global SST products generated only once per day.

7. SUMMARY

This paper describes an experimental design for evaluating the differences between daily regional simulations of a Control configuration initialized with interpolated land surface data from the NCEP Eta model (Control) versus the same model setup initialized with high-resolution land surface data from the NASA LIS (LISWRF), as well as MODIS SST composites (LISMOD). Fifty-eight individual daily simulations were generated for the Control, LISWRF, and LISMOD experimental configurations during May 2004 over Florida and surrounding areas, 29 initialized at 0000 UTC and another 29 initialized at 1200 UTC. The initial soil conditions in the LISWRF simulations came from an offline run of the Noah LSM within the LIS software for 2 years prior to the beginning of the month-long period of study. Atmospheric variables used for forcing the Noah LSM during the offline integration were provided by a combination of NLDAS and GDAS gridded analyses.

Comparisons between the Control and LISWRF runs from 6 May 2004 suggested that the high-resolution soil initial conditions provided by LIS improved the timing and evolution of a sea-breeze circulation over portions of northwestern Florida compared to the Control simulation. The LISWRF model run produced an area of warmer simulated 2-m temperatures over parts of northern Florida and southern Georgia, which resulted in an enhanced land-sea temperature contrast and correspondingly stronger and faster-moving sea-breeze front. The faster sea-breeze solution in LISWRF verified more favorably than the Control at multiple locations in NW Florida.

The LISWRF and LISMOD runs produced a more amplified diurnal range in 2-m temperatures compared to the Control due to the drier initial LIS soil states. This increased diurnal temperature range in LISWRF came from a reduction in the nocturnal warm bias in conjunction with a reduction in the daytime cold bias, and was more inline with observations. Daytime LISWRF and LISMOD dewpoints over land were correspondingly drier than the Control dewpoints, again a manifestation of the drier initial soil state provided by LIS. Most other verified quantities indicated little improvement over the Control simulations.

The LISMOD error statistics were generally quite similar to the LISWRF errors, especially over land. The MODIS SSTs were consistently cooler at the verified marine stations. The SST biases for all experiments indicated a diurnal trend of ~0.5–1.0°C in the observed SSTs, suggesting that SST variations may be important in local and regional modeling applications, even on diurnal time scales.

8. ACKNOWLEDGEMENTS/DISCLAIMER

Mention of a copyrighted, trademarked or proprietary product, service, or document does not constitute endorsement thereof by the authors, ENSCO Inc., the SPoRT Center, the National Aeronautics and Space Administration, or the United States Government. Any such mention is solely for the purpose of fully informing the reader of the resources used to conduct the work reported herein.

9. REFERENCES

Briegleb, B. P., P. Minnis, V. Ramanathan, and E. Harrison, 1986: Comparison of regional clear-sky albedos inferred from satellite observations and model computations. *J. Climate Appl. Meteor.,* **25,** 214-226.

Case, J. L., W. L. Crosson, S. V. Kumar, W. M. Lapenta, and C. D. Peters-Lidard, 2007a: Impacts of High-Resolution Land Surface Initialization on Regional Sensible Weather Forecasts from the WRF Model. *Submitted to J. Hydrometeor.*

Case, J. L., K. M. LaCasse, J. A. Santanello, W. M. Lapenta, and C. D. Peters-Lidard, 2007b: Improved modeling of land-atmosphere interactions using a coupled version of WRF with the Land Information System. Preprints, *21st Conf. on Hydrology,* San Antonio, TX, Amer. Meteor. Soc., 5A.4. [Available online at http://ams.confex.com/ams/pdfpapers/116826.pdf]

Chen, F., and J. Dudhia, 2001: Coupling an advanced land-surface/hydrology model with the Penn State/NCAR MM5 modeling system. Part I: Model implementation and sensitivity. *Mon. Wea. Rev.,* **129,** 569-585.

Chen, F., and Coauthors, 2007: Description and evaluation of the characteristics of the NCAR High-Resolution Land Data Assimilation System. *J. Appl. Meteor. Climatol.,* **46,** 694-713.

Derber, J. C., D. F. Parrish, and S. J. Lord, 1991: The new global operational analysis system at the National Meteorological Center. *Wea. Forecasting,* **6,** 538-547.

Dudhia, J., 1989: Numerical study of convection observed during the winter monsoon experiment using a mesoscale two-dimensional model. *J. Atmos. Sci.*, **46**, 3077-3107.

Gutman, G. and A. Ignatov, 1998: Derivation of green vegetation fraction from NOAA/AVHRR for use in numerical weather prediction models. *Int. J. Remote Sensing*, **19**, 1533-1543.

Haines, S. L., G. J. Jedlovec, and S. M. Lazarus, 2007: A MODIS sea surface temperature composite for regional applications. *IEEE Trans. Geosci. Remote Sens.*, **45**, 2919-2927.

Hong, S.-Y., J. Dudhia, and S.-H. Chen, 2004: A Revised Approach to Ice Microphysical Processes for the Bulk Parameterization of Clouds and Precipitation, *Mon. Wea. Rev.*, **132**, 103–120.

Janjić, Z. I., 1990: The step-mountain coordinate: Physical package. *Mon. Wea. Rev.*, **118**, 1429–1443.

Janjić, Z. I., 1996: The surface layer in the NCEP Eta Model. Preprints, *Eleventh Conference on Numerical Weather Prediction*, Norfolk, VA, Amer. Meteor. Soc., 354–355.

Janjić, Z. I., 2002: Nonsingular Implementation of the Mellor–Yamada Level 2.5 Scheme in the NCEP Meso model, NCEP Office Note, No. 437, 61 pp.

Kain, J. S., 2004: The Kain-Fritsch convective parameterization: An update. *J. Appl. Meteor.*, **43**, 170-181.

Koster, R., and M. Suarez, 1996: Energy and water balance calculations in the mosaic LSM. Technical Memorandum 104606, NASA Goddard Space Flight Center.

Kumar, S. V., and Coauthors, 2006. Land Information System – An Interoperable Framework for High Resolution Land Surface Modeling. *Environmental Modeling & Software*, **21** **(10)**, 1402-1415, doi:10.1016/j.envsoft.2005.07.004.

Kumar, S. V., C. D. Peters-Lidard, J. L. Eastman, and W.-K. Tao, 2007a: An integrated high-resolution hydrometeorological modeling testbed using LIS and WRF. *Environmental Modeling & Software*, **23** **(2)**, 169-181, doi: 10.1016/j.envsoft.2007.05.012.

Kumar, S. V., and Coauthors, 2007b: A land surface data assimilation framework using the Land Information System: Description and Applications, *Advances in Water Resources, In review.*

LaCasse, K. M., M. E. Splitt, S. M. Lazarus, and W. M. Lapenta, 2007: The impact of high resolution sea surface temperatures on short-term model simulations of the nocturnal Florida marine boundary layer. *Mon Wea. Rev., In Press.*

Liang, X., D. Lettenmaier, and E. Wood, 1996: One-dimensional statistical dynamic representation of subgrid spatial variability of precipitation in the two-layer variable infiltration capacity model. *J. Geophys. Res.*, **101 (D16)**, 21403-21422.

Liang, X., D. Lettenmaier, E. Wood, and S. Burges, 1994: A simple hydrologically based model of land surface water and energy fluxes for GCMs. *J. Geophys. Res.*, **99 (D7)**, 14415-14428.

Miller, D. A. and R. A. White, 1998: A Conterminous United States multi-layer soil characteristics data set for regional climate and hydrology modeling. *Earth Interactions*, 2. [Available on-line at http://EarthInteractions.org].

Mitchell, K. E., and Coauthors, 2004: The multi-institution North American Land Data Assimilation System (NLDAS): Utilization of multiple GCIP products and partners in a continental distributed hydrological modeling system. *J. Geophys. Res.*, **109**, D07S90, doi:10.1029/2003JD003823.

Mlawer, E. J., S. J. Taubman, P. D. Brown, M. J. Iacono, and S. A. Clough, 1997: Radiative transfer for inhomogeneous atmosphere: RRTM, a validated correlated-k model for the long-wave. *J. Geophys. Res.*, **102 (D14)**, 16663-16682.

Peters-Lidard, C. D., S. Kumar, Y. Tian, J. L. Eastman, and P. Houser, 2004. Global Urban-Scale Land-Atmosphere Modeling with the Land Information System. Preprints, *Symp. on Planning, Nowcasting, and Forecasting in the Urban Zone*, Seattle, WA, Amer. Meteor. Soc., 4.1. [Available online at http://ams.confex.com/ams/pdfpapers/73726.pdf]

Robinson, D. A. and G. Kukla, 1985: Maximum surface albedo of seasonally snow covered lands in the Northern Hemisphere. *J. Climate Appl. Meteor.*, **24**, 402-411.

Rodell, M., P. R. Houser, A. A. Berg, and J. S. Famiglietti, 2005: Evaluation of 10 methods for initializing a land surface model. *J. Hydrometeor.*, **6**, 146-155.

Sellers, P. J., Y. Mintz, and A. Dalcher, 1986: A simple biosphere model (SiB) for use within general circulation models. *J. Atmos. Sci.*, **43**, 505-531.

Skamarock, W. C., J. B. Klemp, J. Dudhia, D. O. Gill, D. M Barker, W. Wang and J. G. Powers, 2005: A Description of the Advanced Research WRF Version 2, NCAR Tech Note, NCAR/TN–468+STR, 88 pp. [Available from UCAR Communications, P.O. Box 3000, Boulder, CO, 80307; on-line at: http://box.mmm.ucar.edu/wrf/users/docs/arw_v2.pdf]

Smagorinsky J., S. Manabe, and J. L. Holloway Jr., 1965: Numerical results from a nine-level general circulation model of the atmosphere. *Mon. Wea. Rev*, **93**, 727–768.

Steenburgh, W. J., S. F. Halvorson, and D. J. Onton, 2000: Climatology of lake-effect snowstorms of the Great Salt Lake. *Mon. Wea. Rev.*, **128**, 709-727.

Sud, Y., and D. Mocko, 1999: New snow-physics to complement SSiB. Part I: Design and evaluation with ISLSCP initiative I datasets. *J. Meteor. Soc. Jap.*, **77 (1B)**, 335-348.

Zobler, L., 1986: A World Soil File for Global Climate Modeling. NASA Technical Memorandum 87802, National Aeronautics and Space Administration, Washington D.C., 32 pp.
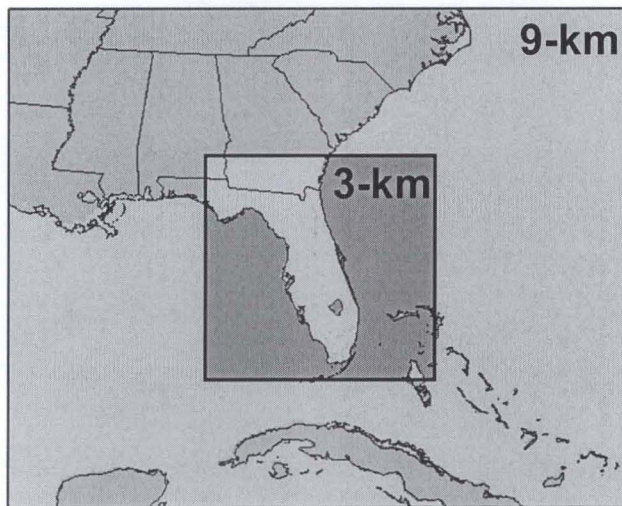

Figure 1. Domain configuration of the simulation experiments for May 2004. The outer grid consists of 250 x 200 mass points in the zonal and meridional directions, respectively, and 9-km horizontal grid spacing. The inner nest contains 279 x 267 mass points and 3-km horizontal grid spacing.
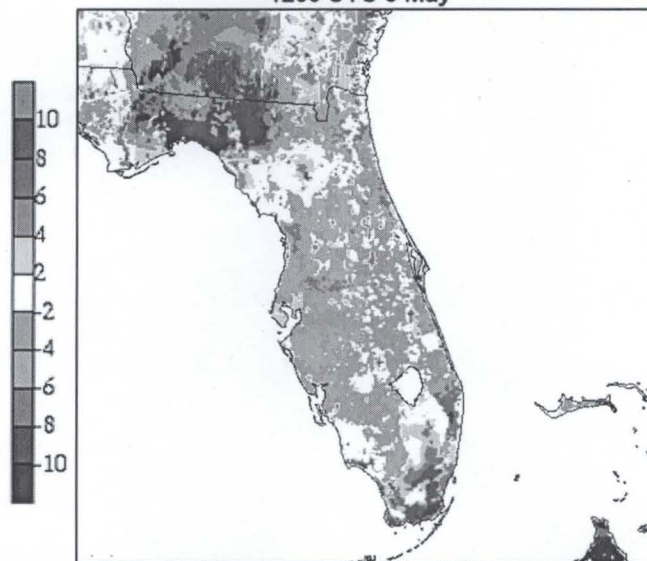

Figure 2. Initial 0–10 cm volumetric soil moisture difference between the LIS and Control (%) on 1200 UTC 6 May 2004.
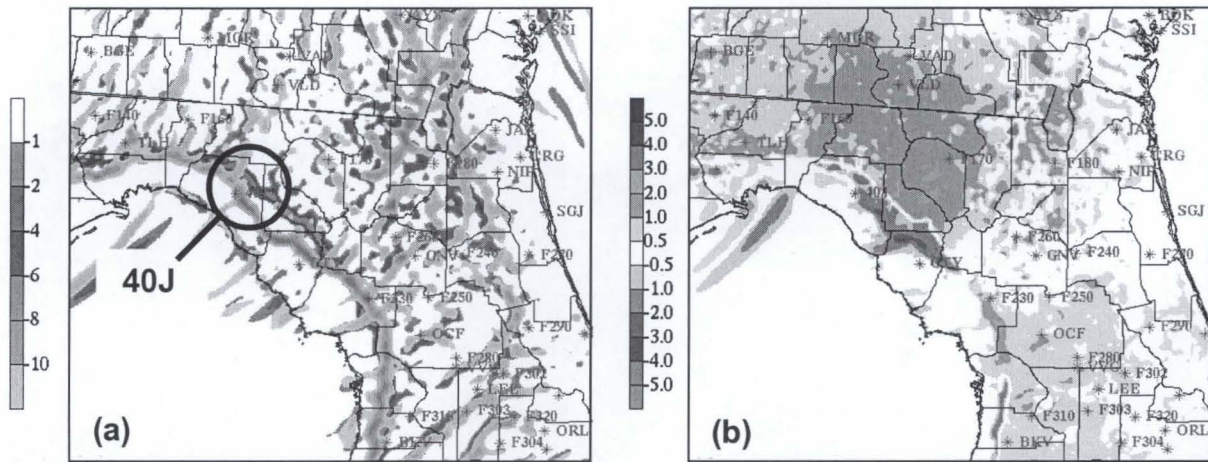
Figure 3. The 1200 UTC 6 May 2004 11-hour forecast of (a) 10-m divergence (x 10^4 s^{-1}; color indicating LISWRF convergence and gray shading indicating Control convergence), and 2-m temperature differences (°C, LISWRF – Control).
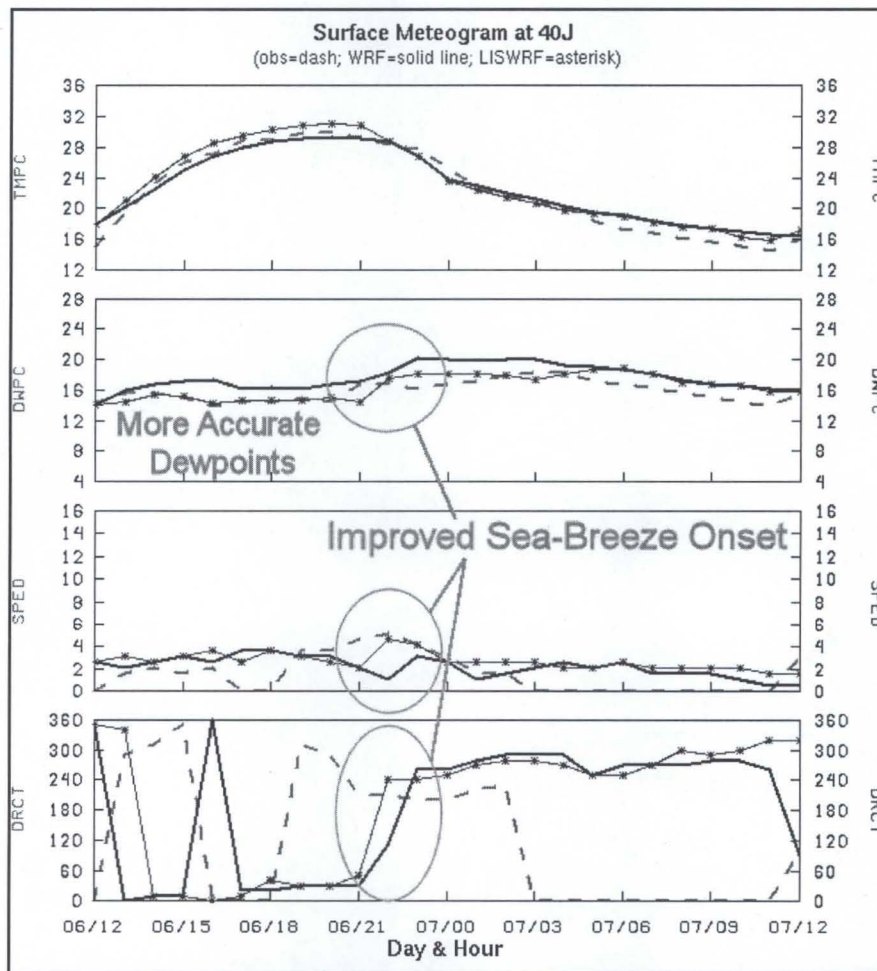

Figure 4. A meteogram plot at Perry, FL (40J) of temperature (°C), dewpoint (°C), wind speed (m s^{-1}), and wind direction (degrees). The graphs compare hourly WRF forecasts interpolated to the station location from the Control simulation (solid line) and LISWRF run (solid line with asterisks) to observations (dashed line).
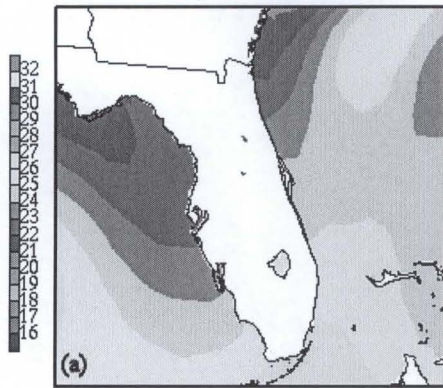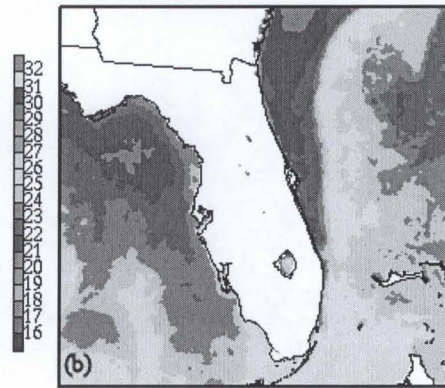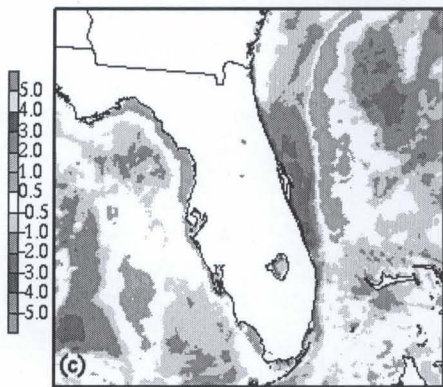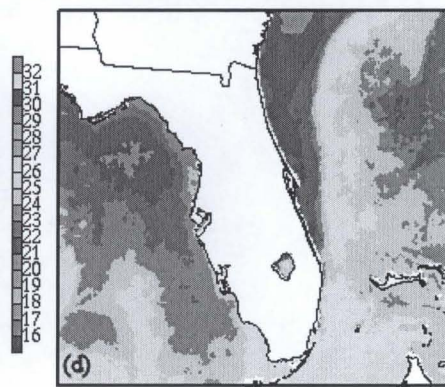
Figure 5. Initial SST fields (°C) valid at 1200 UTC 6 May for (a) the LISWRF run (i.e. Eta SSTs), (b) the LISMOD run (MODIS SSTs), (c) difference between MODIS and Eta SSTs, and (d) the raw 3-km MODIS composite at 0700 UTC prior to interpolation to the WRF grid.

Surface Verification Sites
(star=METAR, triangle=FAWN, box=MARINE)
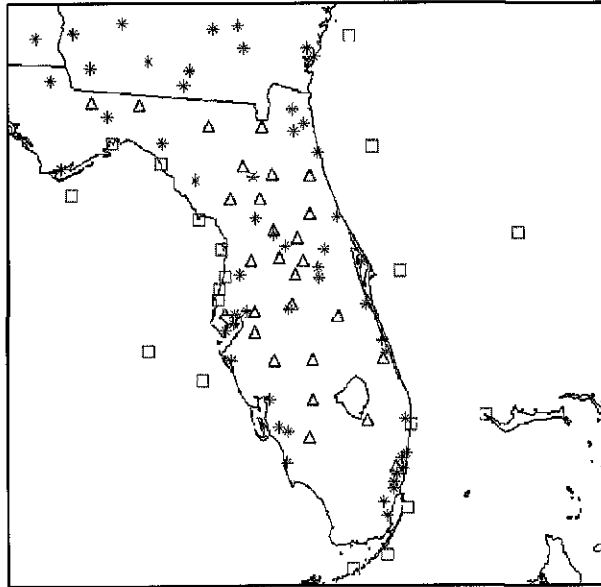
Figure 6. Surface stations used for verification of WRF model forecasts, including land stations [METAR (stars) and FAWN (triangles)], and marine/water sites [buoys and Coastal-Marine Automated Network (C-MAN) represented by boxes].
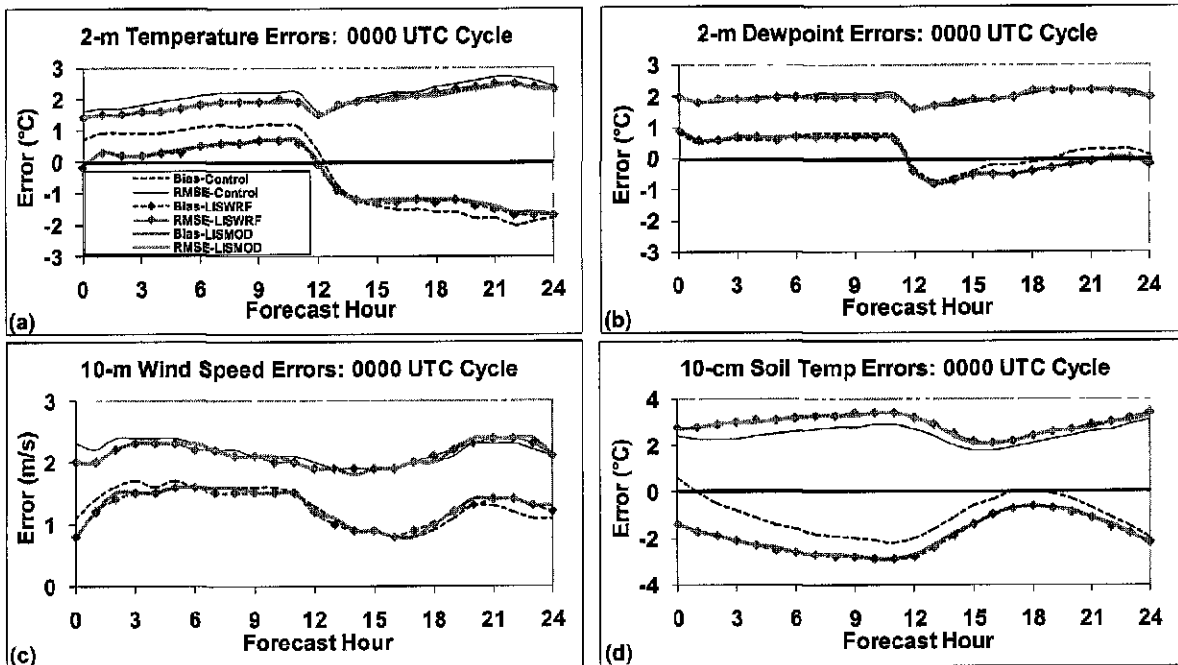

Figure 7. Surface verification statistics for the 0000 UTC WRF forecast cycle for the land stations depicted in Figure 6 for the variables (a) 2-m temperature, (b) 2-m dewpoint, (c) 10-m wind speed, and (d) 10-cm soil temperature (FAWN sites only). The legend in panel (a) indicates the plot associated with each experiment type.
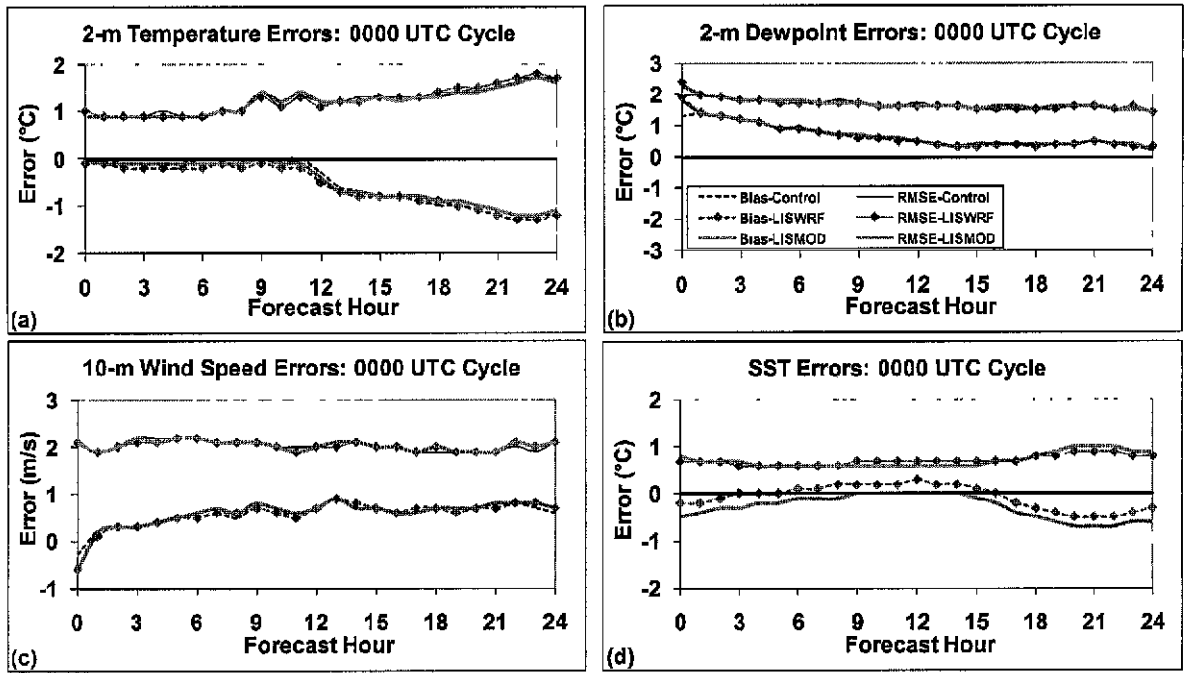
Figure 8. Surface verification statistics for the 0000 UTC WRF forecast cycle for the marine stations depicted in Figure 6 for the variables (a) 2-m temperature, (b) 2-m dewpoint, (c) 10-m wind speed, and (d) sea surface temperature (SST). The legend in panel (a) indicates the plot associated with each experiment type.